Talanta 126 (2014) 27–37

Contents lists available at ScienceDirect

Talanta

journal homepage: www.elsevier.com/locate/talanta

Graphene coated silica applied for high ionization matrix assisted laser desorption/ionization mass spectrometry: A novel approach for environmental and biomolecule analysis ☆

Hani Nasser Abdelhamid [a,b], Bo-Sgum Wu [a], Hui-Fen Wu [a,c,d,e,f,*]

[a] Department of Chemistry, National Sun Yat-Sen University, Kaohsiung 804, Taiwan
[b] Department of Chemistry, Assuit University, Assuit 71515, Egypt
[c] College of Pharmacy, Kaohsiung Medical University, Kaohsiung 807, Taiwan
[d] Center for Nanoscience and Nanotechnology, National Sun Yat-Sen University, Kaohsiung 804, Taiwan
[e] Institute of Medical Science and Technology, National Sun Yat-Sen University, 80424 Taiwan
[f] Doctoral Degree Program in Marine Biotechnology, National Sun Yat-Sen University, Kaohsiung 804, Taiwan

ARTICLE INFO

Article history:
Received 23 January 2014
Received in revised form
7 March 2014
Accepted 10 March 2014
Available online 18 March 2014

Keywords:
Graphene
Silica
Surface assisted laser desorption/ionization (SALDI)
Surfactant

ABSTRACT

The integration of nanotechnology with mass spectrometry for sensitive and selective detection of molecules is a hot/important field of research. Synthesis of graphene (G) coated with mesoporous silica (SiO_2, G@SiO_2) for mass spectrometric application has been demonstrated. For the first time, we proposed the significant role of surfactant that used during the synthesis of mesorporous silicate (SiO_2) in mass spectrometry. It was noticed that G could initiate SiO_2 via surfactants which work as initiators for further ionization. The porosity of SiO_2 trapped the analytes that was released and ionized with the surfactant fragments. Undoubtedly, strong background interferences were present in the case of organic matrix, which greatly obscured the detection of low molecular weight compounds. G@SiO_2 nanocomposite affords several advantages, such as the ability to detect small molecules (<500 Da), high sample localization through silica mesoporosity, and high ionization efficiency over than G or conventional matrices. The high performance of G@SiO_2 is not only due to the large surface area but also due to high desorption/ionization efficiency of inevitably surfactant (cetyltrimethylammonium chloride, CATB). Unlike the conventional MALDI-MS, the G@SiO_2-MS is capable of generating multiply charged polysaccharides. The present method was validated to detect surfactants with low limits of detection.

1. Introduction

Matrix-assisted laser desorption ionization mass spectrometry (MALDI–MS) is a soft ionization technique which could be applied for non-volatile molecule analysis [1]. However, it is difficult to detect low molecular weight (LMW) compounds (MW < 1000 Da), because common MALDI matrices which are typically from low molecular weight organics acids produce matrix-related ions which show strong interferences at low mass regions (MW < 1000 Da) [2,3]. Therefore, nanomaterials are attractive matrix subjects in MALDI-MS because of their promising features in applications and less interference. Various nanomaterials have been successfully applied in surface assisted laser desorption/ionization mass spectrometry (SALDI-MS) [4–10]. Commercial silylated silicon nanowires was used in laser desorption mass spectrometry (LDI-MS) and called as nano-assisted laser desorption/ionization (NALDI-MS [11]. Polymer-assisted laser desorption/ionization mass spectrometry (PALDI-MS), based on small polymers as nonpolar matrices, was proposed [12]. A type of LDI-MS using sol–gel as matrix, called sol–gel-assisted laser desorption/ionization (SGALDI) mass spectrometry was also reported [13]. It is important to note that direct laser desorption/ionization (matrix-free) from various surfaces have been applied extensively [14,15]. Recently, matrix surfactant-suppressed laser desorption/ionization (MSLDI-MS [16] was successfully employed in the analysis of small molecules via the addition of cetyltrimethylammonium bromide (CTAB) which can suppress ions of the conventional matrix.

Graphene (G) is truly the material of the moment since 2004 [17]. It is composed from a single layer of carbon atoms (sp^2–sp^2) that can be prepared from graphite [17]. Thus, G was utilized as MALDI matrix to detect low-mass molecules, such as amino acids, polyamines, peptides, steroids, nucleosides, nucleotides, metals and metallodrugs [18–24]. The analytical application of G was reviewed [25]. Soft-landing using MALDI-MS (bottom–up growth) of polycrystalline layered ultrathin films to produce ultrapure ordered architectures of giant G nanosheet was reported [26]. Recently, G was used as a template to control the microstructure of mesoporous silica (SiO_2)

☆Contract/grant sponsor: National Science Council Taiwan
* Corresponding author at: Department of Chemistry, National Sun Yat-Sen University, Kaohsiung, 804, Taiwan. Tel.: +886 7525 2000 3955; fax: +886 7525 3908.
E-mail address: hwu@faculty.nsysu.edu.tw (H.-F. Wu).

http://dx.doi.org/10.1016/j.talanta.2014.03.016
0039-9140/

[27]. G shows high sensitivity, and low interference (< 1000 Da) in LDI-MS, but it shows low resolution due to interaction with aromatic compounds (π–π interactions), and has low stability due to van der Waals forces.

In this article, we describe an efficient method for synthesis of G@SiO_2 nanosheets using ultrasonication. The unique porous silica layer modified on the surface of G plays many function such as: (1) localize the analyte into the porous cavity and prevent analyte delocalization, (2) decrease analyte fragmentation due to large surface area of G, (3) effectively prevent the irreversible aggregation of G and (4) decrease high interaction of analyte with G nanosheet, for instance aromatic compounds that interact via π–π interactions.

2. Experimental section

2.1. Materials and methods

Acetonitrile, trifluoroacetic acid (TFA), 1-butyl-3-methyl-imidazolium chloride and polyethylene glycol "PEG 200" were chromatographic grade (Merck, Darmstadt, Germany). Cetyl pyridinium chloride monohydrate, tetramethyl ammonium hydroxide pentahydrate, cetyltrimethylammonium chloride, gramicidin D, β-cyclodextrin, maltoheptose, gentobiose, palatinose, panose, tobramycin, spectinomycin and sodium dodecyl sulfate were purchased from Sigma, Switzerland. Sucrose was purchased from J.T. Baker, USA. Double distilled water was purified by Milli-Q system (18 ΩM, USA).

2.2. MALDI-TOF mass spectrometer

The MALDI-TOF mass spectra were obtained from Microflex (Bruker, Germany). The instrument was equipped with a nitrogen laser (λ=337 nm) and time of flight (TOF) tube (1.25 m) with average laser shots 100 shots. The accelerating voltage used was 19 kV. A stainless steel target (96 spots) was used as the MALDI substrate on which the samples are deposited. All mass spectra were obtained in the positive-ion reflectron mode. All analytes are repeated three times to confirm repeatability.

2.3. Characterization instruments

G@SiO_2 was characterized using transmission electron microscopy (TEM) (Philips CM200, Switzerland), operated at 300 keV. Fourier transform infrared (FT-IR) measurements were carried out at room temperature on a Perkin-Elmer Spectrum 100FT-IR. UV measurements were carried out using the Perkin Elmer lambda 20.

2.4. Preparation of SiO_2 on G

G was synthesized from natural graphite flakes by the Hummer's method [21,28] and G@SiO_2 sheets were fabricated by a modification from the approaches [25,27] to avoid surfactants. In a typical experiment, porous silica was prepared via acoustic precipitation of 0.25 mL of tetraethylorthosilicate (TEOS) suspended in an aqueous solution containing CTAB (1 g) and NaOH (40 mg), after magnetic stirring for 2 h at 80 °C. The precipitate was washed several times to remove all possible surfactant (CTAB) using water and aqueous methanol. Equal weight of G (0.2 g) and silica (0.2 g) were dispersed in 15 mL deionized water and subjected to sonication for 24 h.

2.5. Sample preparation

All samples were spotted onto the MALDI plates using the dry-droplet method. Briefly, about 10 μL of G@SiO_2 and 10 μL of different analytes were mixed together. About 2 μL of the mixture was spotted into MALDI plate and kept in room temperature prior to drying. The sample plate was finally loaded into the ion source for analysis.

3. Result and discussion

3.1. Characterization of G@SiO_2 nanocomposite

The G@porous silica (G@SiO_2) sheets were fabricated via sonication of silica nanoparticles with G nanosheet. G is prepared using the Hummer's method [28]. The morphology and structure of the prepared G and G@SiO_2 sheets were investigated via TEM as shown in Fig. 1 (A–C). Fig. 1A shows G as long transparent nanosheet. Large porous silica layer is attached strongly to G nanosheet (Fig. 1B) that can be clearly observed in the TEM magnification (Fig. 1C). The UV spectrum (Fig. 1D) shows continuous absorption that covers wide ranges of wavelengths, so that it can assist desorption/ionization of different analytes. The porous silica layer shows no change in fluorescence emission of G (Fig. 1E) at the excitation wavelength 270 nm. While, G is transparent in FTIR, G@SiO_2 shows strong peaks at wavenumber (cm^{-1}), 3450 and 1000 corresponding to O–H and –Si–O–, respectively (Fig. 1F). Peaks at 1000 cm^{-1} (Si–O) confirm coating of G by SiO_2 layer.

3.2. G and G@$SiO_2$for biomolecules analysis

Various biomolecules belong to peptide (gramicidin D (2 μL, 2 fmol), polymer (polyethylene glycol "PEG" (2 μL, 2 pmol), maltoheptose (2 μL, 20 pmol)), β-cyclodextrin (2 μL, 2 fmol), carbohydrate (gentiobiose (2 μL, 10 fmol)), palatinose (2 μL, 20 pmol)), pannose (2 μL, 10 fmol)), sucrose (2 μL, 10 fmol))) and drugs (tobramycin (2 μL, 10 fmol), spectinomycin (2 μL, 10 fmol)) were tested in Fig. S1.

Gramicidin D (GD) is a linear pentadecapeptide with molecular formula $C_{99}H_{140}N_{20}O_{17}$ and molecular mass 1882.3 g/mol. Mass spectra (Fig. 2A) using DHB, G and G@SiO_2 of GD show protonated peak at 1882.0 Da corresponding to the protonated GD i.e $[GA+H]^+$. In contract with G; G@SiO_2 exhibits a clear background with high intensity of protonated peak i.e $[GA+H]^+$. The reason may be due to strong interaction between negative charge of G and the positive charge on GD. The peaks at *m/z* 1905.0 and 1921.0 Da corresponding to $[GA+Na]^+$ and $[GA+K]^+$. Conventional matrix (DHB) shows no limitation in GD analysis as it has high mass which not submerged with matrix ions.

β-cyclodextrin has molecular mass 1135.0 g/mol. Fig. 2B shows peaks at *m/z* 1158.0 and 1174.6 Da corresponding to $[\beta Cy+Na]^+$ and $[\beta Cy+K]^+$, respectively. Due to the low interaction between β-cyclodextrin with G@SiO_2 and localization of the molecules in the porous cavity, it shows low fragmentation (Fig. 2B). Gramicidin and cyclodextrin can be ionized by the conventional organic matrices due to higher in molecular weight. However, we tested these compounds to check the ionization ability of G and G@SiO_2 to work as matrices for higher molecular weight analytes (M. Wt < 3000 Da) and the results show that G@SiO_2 offers higher performance over than G alone.

Polyethylene glycol "PEG 200" is a polyether compound with chemical formula $C_{2n}H_{4n+2}O_{n+1}$ and variable molecular mass. It has many applications from industrial manufacturing to biomedicine and biotechnology. Conventional matrix "DHB" displays a lot of interferences at low *m/z*, while G and G@SiO_2exhibit no interference. Furthermore, G@SiO_2shows high ionization efficiency comparing to G alone at *m/z* > 500 Da (Fig. 3A).

Maltoheptose is an oligosaccharide with chemical formula $C_{42}H_{72}O_{36}\cdot xH_2O$ and molecular mass 1153.0 Da. MALDI-MS spectra (Fig. 3B) show peaks at *m/z* 1153.0, 1176.7 and 1192.0 Da corresponding to $[Malt+H]^+$, $[Malt+K]^+$ and $[Malt+K]^+$. G

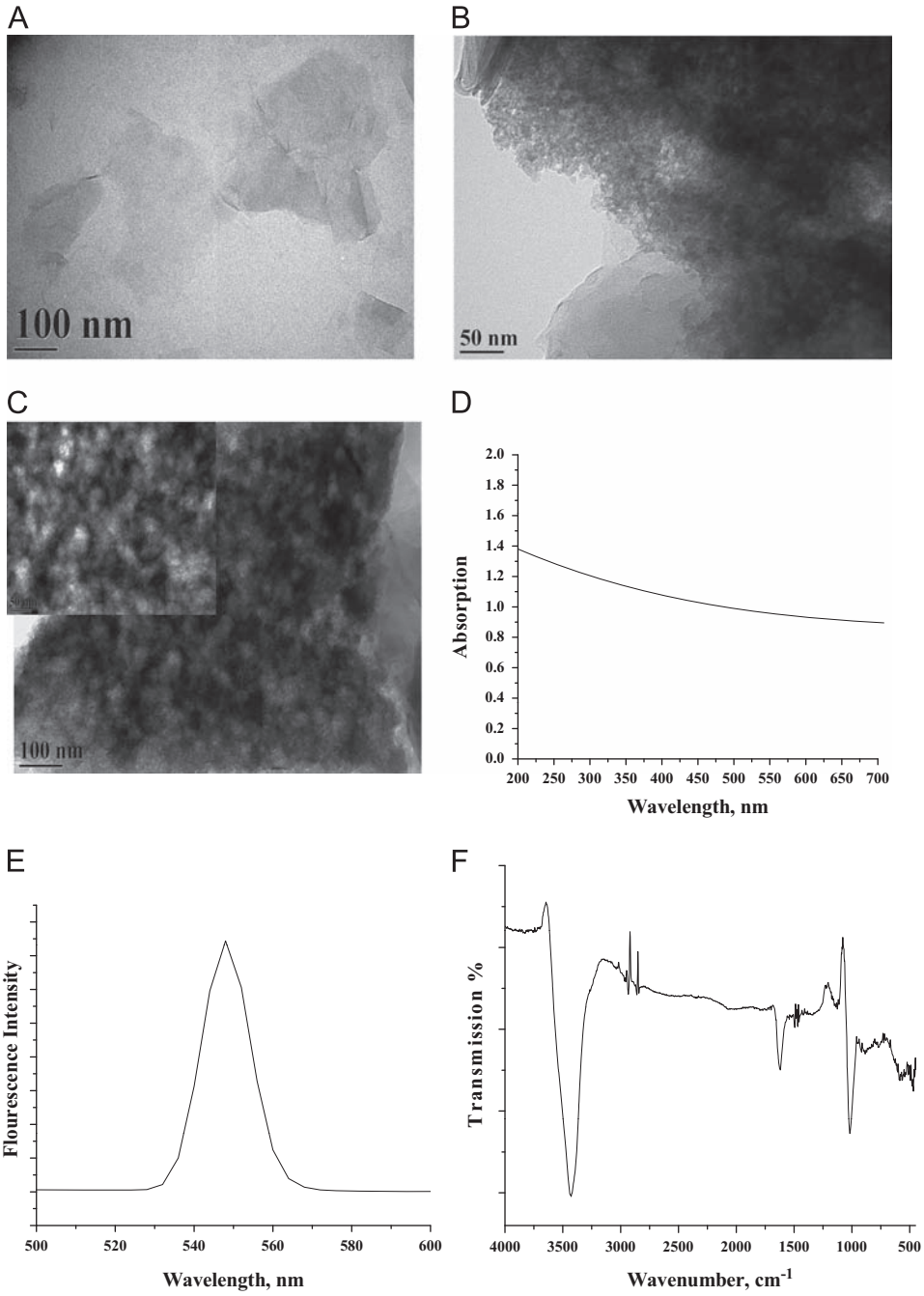

Fig. 1. Characterization of G and G@SiO_2. TEM image of (A) G, (B) G@SiO_2 and (C) magnification of G@SiO_2 that show porosity, (D) UV absorption of G@SiO_2, (E) fluorescence spectra at excitation wavelength 270 nm, and (F) FTIR spectrum of G@SiO_2.

based material shows ionization of the protonated peak, while conventional matrix (DHB) ionized the compound via cationization due to secondary ionization. In the other hand, G@SiO_2displays high ionization efficiency comparing to G. A homemade MALDI-MS was used to frozen 2,5-dihydroxybenzoic acid at 100 K for maltoheptose and polysaccharide analysis [29]. G@SiO_2 shows almost the same results without the necessity to use new instrument or low temperature. Unlike conventional MALDI-MS, the G@SiO_2-MS is capable of generating multiply charged polysaccharides similar to cryo-MALDI-MS [29].

Gentiobiose, palatinose and sucrose are disaccharide composed of two units of glucose with molar mass 342.3 g/mol, except sucrose composed of glucose and fructose moieties. MALDI-MS spectra of gentobiose (Fig. 4A) exhibits peaks at *m/z* 365.0, 381.2 and 441.5 Da corresponding to $[Gent+Na]^+$, $[Gent+K]^+$, and $[(Gent\text{-}2H)+2K+Na]^+$, respectively. While the spectra of palatinose (Fig. 4B), sucrose (Fig. S2A) disclose a main peak at 365.0 Da corresponding to $[Pala+Na]^+$ and $[Sucr+Na]^+$. G@SiO_2 produces low interferences with low fragmentation due to weak interaction with G sheet. Astonishing peaks above 600 Da are observed in the case of sucrose with G. A series of reproducible peaks with difference 24 Da are recorded (Fig. S2A), it may due to the formation of porous carbon of sucrose using silica as template after irradiated with laser radiations. In contrast, using DHB as the matrix, we can visualize a lot of interferences in the spectra; so the spectra are ambiguous.

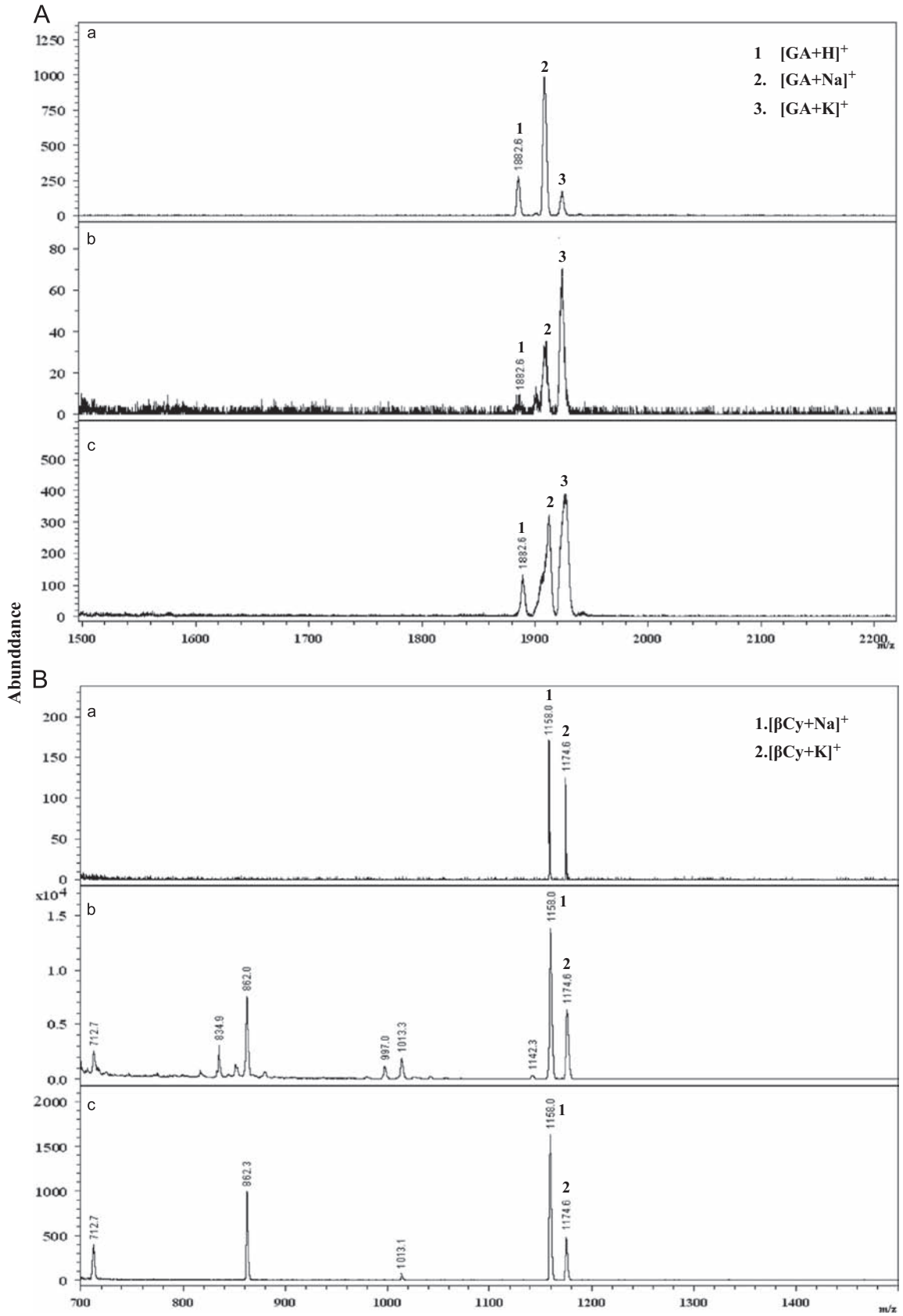

Fig. 2. MALDI spectra of (A) gramicidin D and (B) β-cyclodextrin for (a) DHB, (b) G and (c) G@SiO_2.

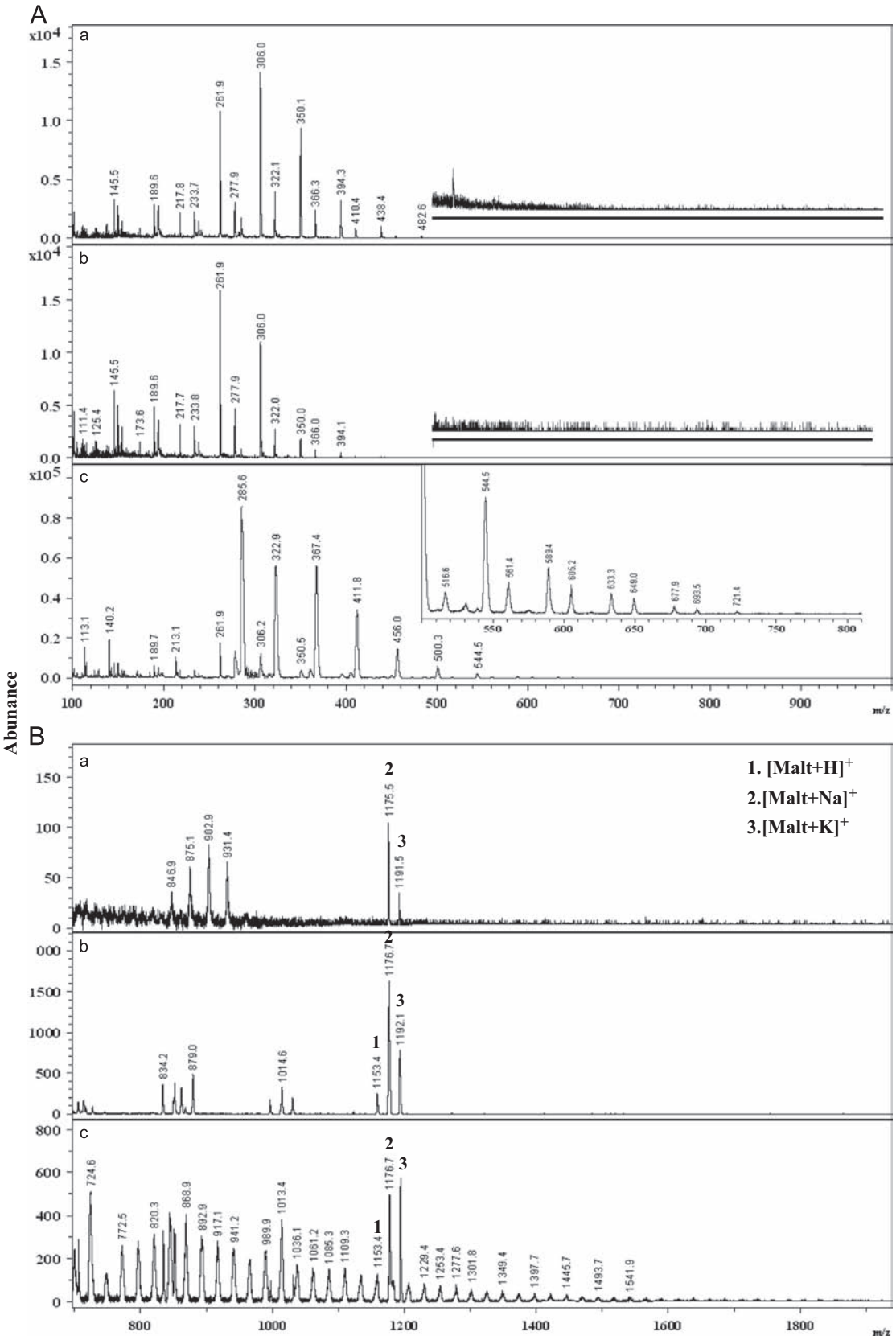

Fig. 3. MALDI spectra of (A) polyethylene glycol and (B) maltoheptose for (a) DHB, (b) G and (c) G@SiO_2.

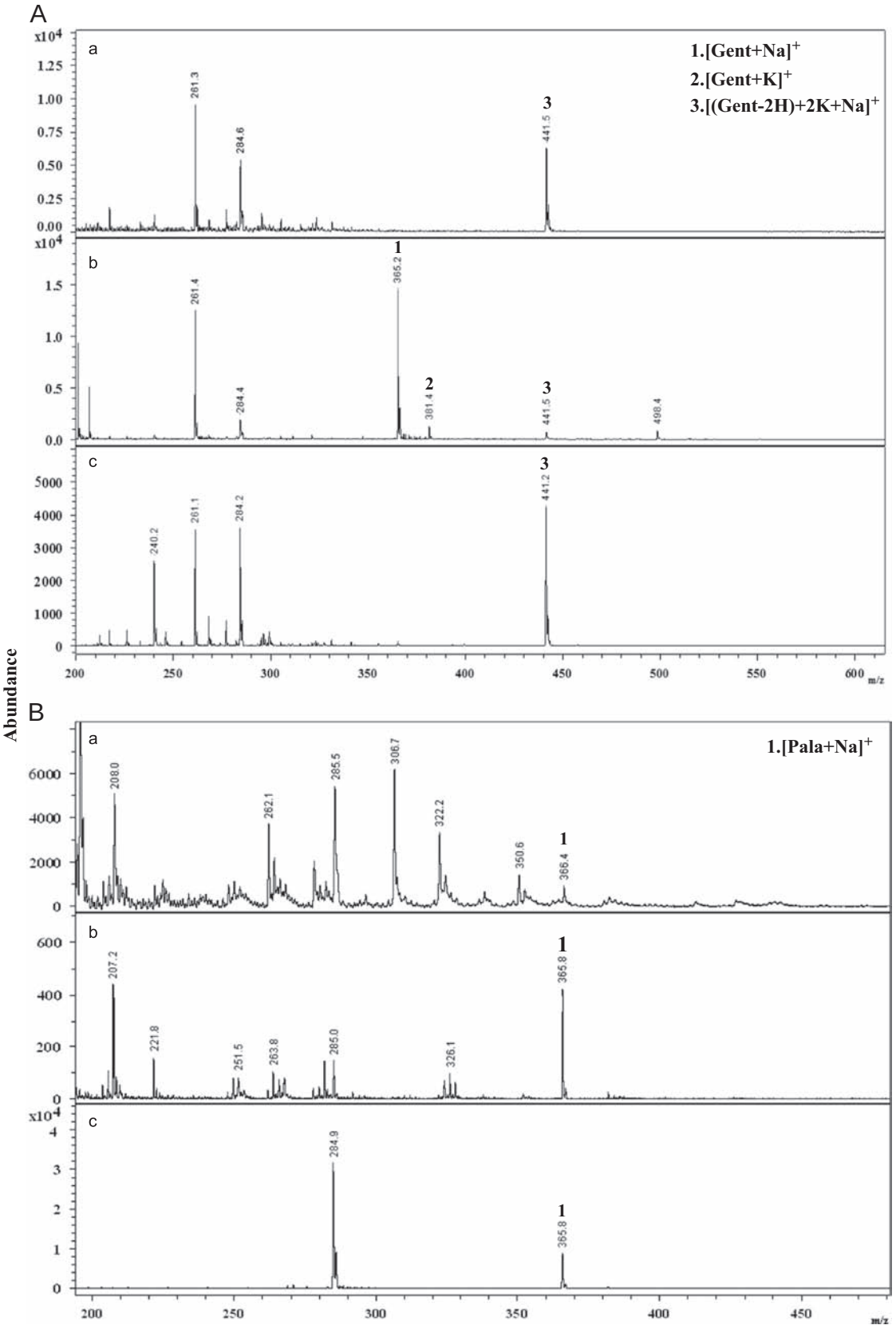

Fig. 4. MALDI spectra of (A) gentobiose and (B) palatinose for (a) DHB, (b) G and (c) G@SiO_2.

Panose is trisaccharide with molar mass 504.4 Da. MALDI-MS spectra in Fig. S2B, supporting file generated peaks at *m/z* 527.0 and 544.1 Da corresponding to $[Pan+Na]^+$ and $[Pan+K]^+$, respectively. The resulting MALDI spectra of G@SiO_2 present better ionization and low interferences than G alone.

3.3. Drug analysis of "tobramycin and spectinomycin"

Tobramycin is an aminoglycoside antibiotic with molar mass 467.5 g/mol. Mass spectra (Fig. S3A) show the sodium peak of the drug at *m/z* 491.0 Da corresponding to $[Tob+Na]^+$.

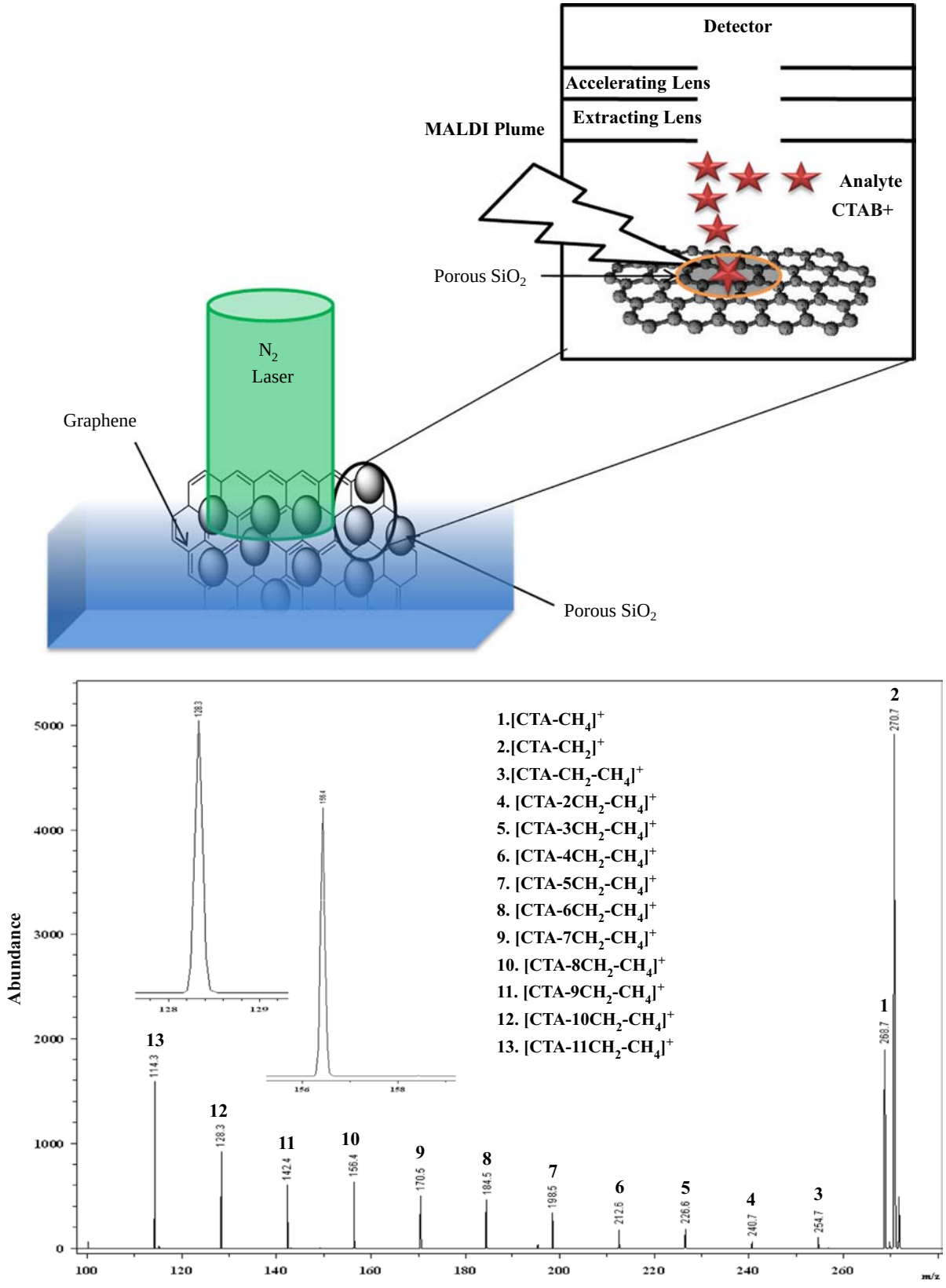

Scheme 1. Laser desorption/ionization of analyte on the surface of G@SiO_2.

Spectinomycin is an aminocyclitol antibiotic with molar mass 332.0 g/mol. The analyte shows peaks at *m/z* 332.2 and 356.5 Da corresponding to $[Spect+H]^+$, and $[Spect+Na]^+$, respectively (Fig. S3B).

Conventional matrix "DHB" displays a lot of matrix-related peaks which increase spectrum ambiguity. In the other side, G and G@SiO_2 exhibits low interferences and low background signals. As stated above, G@SiO_2 offers the lowest interference, as it shows

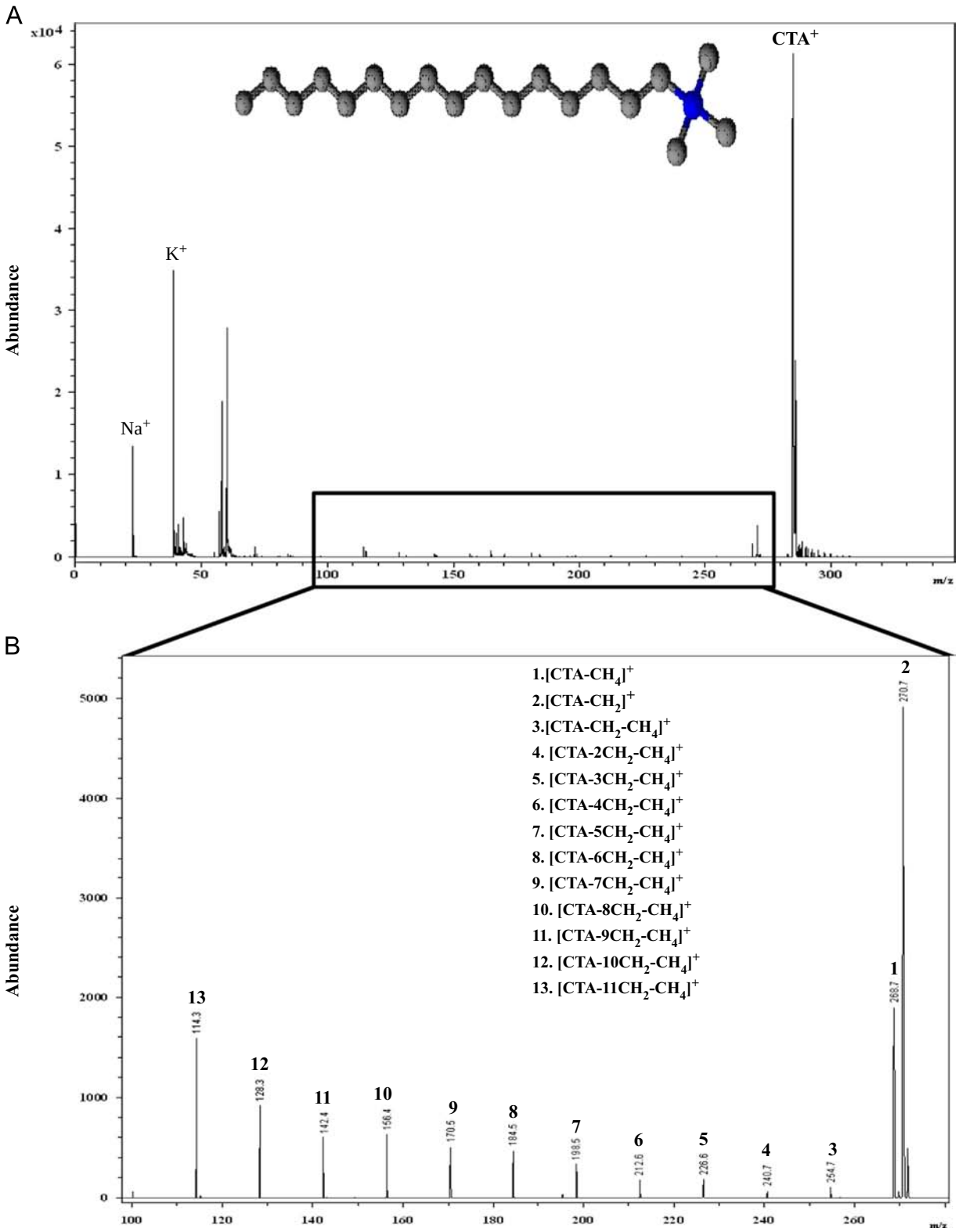

Fig. 5. Mass background of G@SiO_2, (A) Overall view of G@SiO_2, inset represent the chemical structure of CTAB, and (B) intensive observation in mass range *m/z* 100–280. (For interpretation of the references to color in this figure legend, the reader is referred to the web version of this article.)

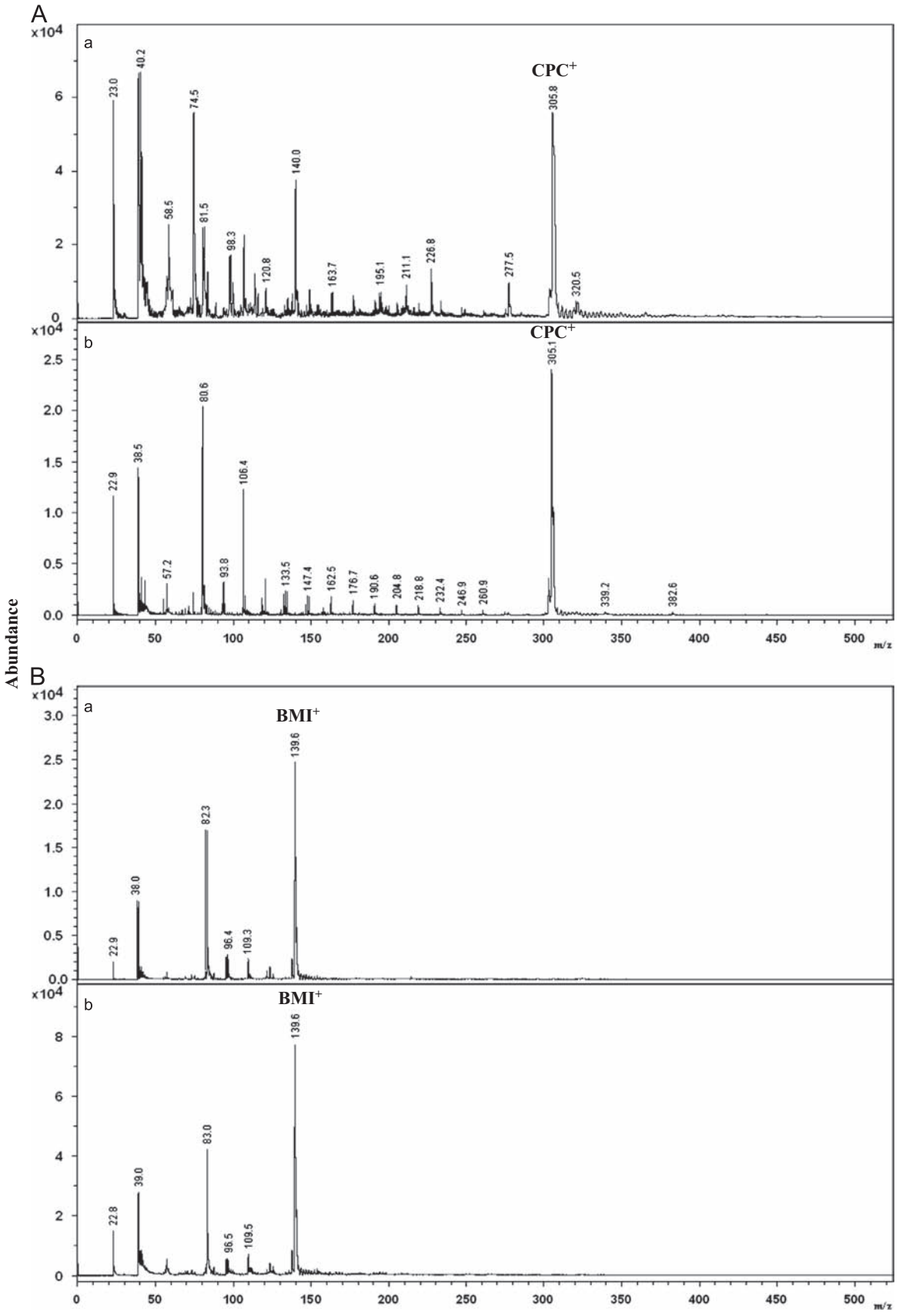

Fig. 6. LDI-MS for (A) cetylpyridinium chloride monohydrate, CPC and (B) 1-butyl-3-methyl-imidazolium chloride, BMI for (a) DHB and (b) G.

only one peak for the ionization of drug (analyte signal) and no peaks related to nanomaterials (interferences).

3.4. Mechanism of high ionization efficiency

Although the possible mechanisms for the laser desertion/ionization (LDI–MS) are still unknown, according to the UV absorption mechanism, the matrix might absorb the UV radiation, enabling to promote desorption and ionization of analytes in the gas phase [30]. Preliminary, the UV spectrum indicates that G@SiO_2 have a strong and continuous absorbing from 200–700 nm (Fig. 1D), while G alone absorbs ultraviolet about 270 nm [18–24]. This observation may be the prime reason why G@SiO_2 shows high performance than G.

The analyte is adsorbed on the top of the G@SiO_2 surface and laser irradiation results rapid surfaces heating causing desorption of adsorbed analytes. High absorption of G assist analyte desorption as shown in the UV spectrum (Fig. 1D). The collisions among ions in the MALDI plume can lead to an energy deficit and impart internal energy, which may lead to metastable decay (broad band) or ion suppression. Thus, little plume gives better resolution [31]. When laser hits G@SiO_2 (Scheme 1A), analyte desorbed from the porous cavity of G@SiO_2, while in case of G, it desorbed from the flat surface. In nanostructurte initiator mass spectrometry (NIMS) that uses a liquid initiator to facilitate desorption. During NIMS desorption/ionization process, the porous silicon absorbs laser radiation that results in rapid surface heating, vaporization of the trapped initiator, and desorption/ionization of the adsorbed analyte without fragmentation [32].

While in this study, both G and SiO_2 participate in desorption process. The rate of desorption in the case of G@SiO_2 is higher than G alone, thus it shows high ionization. The overview of G@SiO_2 background (Fig. 5A) presents peaks at 23, 39, and 284.5 Da corresponding to Na^+, K^+ and CTA^+. However, silica is prepared and washes many times to remove all CTAB; it exists inevitably at negligible concentration. Due to large surface of the G@SiO_2, this trivial amount can be ionized as shown in Fig. 5A. A close observation in the mass range 100–280 Da (Fig. 5B) offers a series of peaks 270.7, 268.7, 254.7, 240.7, 226.6, 212.6, 196.5, 184.5, 170.5, 156.4, 148.3, and 114.3 Da with differences 14 Da corresponding to $[CTA\text{-}CH_2]^+$, $[CTA\text{-}CH_4]^+$, $[CTA\text{-}CH_2\text{-}CH_4]^+$, $[CTA\text{-}2CH_2\text{-}CH_4]^+$, $[CTA\text{-}3CH_2\text{-}CH_4]^+$, $[CTA\text{-}4CH_2\text{-}CH_4]^+$, $[CTA\text{-}5CH_2\text{-}CH_4]^+$, $[CTA\text{-}6CH_2\text{-}CH_4]^+$, $[CTA\text{-}7CH_2\text{-}CH_4]^+$, $[CTA\text{-}8CH_2\text{-}CH_4]^+$, $[CTA\text{-}9CH_2\text{-}CH_4]^+$, $[CTA\text{-}10CH_2\text{-}CH_4]^+$, $[CTA\text{-}11CH_2\text{-}CH_4]^+$, and $[CTA\text{-}12CH_2\text{-}CH_4]^+$, respectively (Fig. 5B). Presences of these ions may be the reason for low fragmentation and high desorption efficiency. Furthermore, G@SiO_2 has high absorption capabilities that localize the analyte via the porosity of silica [32–35]. However, MALDI plume is very crowding by surfactant ions, G@SiO_2 still show ionization of various analytes. These ions can carry the analyte ions without lost of their charges.

Although NIMS is robust, sensitive, it lacks of reproducibility between the various silicon wavers, and it is also expensive, required tedious preparation methods/instrumentations and can be discriminated between analytes that limit its application. While G@SiO_2 is a simple, cheap, and reproducible technique.

In NIMS, a wide range of initiators including lauric acid, polysiloxanes, siloxanes and silanes (molecular masses from 200 to 14,000 Da) have been used. Here, cheap surfactant (CTAB) can work effectively. The presented technique (G@SiO_2-MS) plays a clear distinguish between different isobaric biomolecules (Fig. 4).

3.5. Application of G for surfactant detection

Surfactants have been used intensively nowadays and were considered as a major component of the environmental pollutants [36,37]. Thus, it is paramount important to develop simple, and selective method to monitor the surfactants in water. Many well-known methodologies require tedious procedures, use more hazardous chemicals, show limitations in their applicability, and most commonly related to reproducibility and signal stability [36,37]. Thus, new methodology for sensing or detection of surfactant is necessary [36,37]. So we try to investigate the new method to detect surfactants and to address the real role of G to initiate this ionization. Series of positive surfactant called cetyltrimethylammonium chloride (CTAB, Fig. S4(A, B)), tetramethyl ammonium hydroxide pentahydrate (TMAH, Fig. S5A), tetrabutyl ammonium hydroxide (TBA, Fig. S5B), cetylpyridinium chloride monohydrate (CPC, Fig. 6A), 1-butyl-3-methyl-imidazolium chloride (BMI, Fig. 6B) and sodium dodecyl sulfate (SDS, Fig. S6) were investigated. Spectrum (Fig. S4A) of G and CTAB shows the same pattern of CTAB with G@SiO_2 nanocomposite, but with low resolution due to absence of SiO_2 nanolayer. Thus, SiO_2 displays also a role in the ionization. Among the different surfactant used here, only CPC and CTAB can show series of peaks with 14 Da difference. The peaks assignments are written in the figure of each surfactant. MALDI data indicate that negative charge of G surface plays a role to stabilize the positive charges of surfactant, thus these surfactant exhibits unique peaks pattern with 14 Da corresponding to $–CH_2–$. This negative cloud is decreased when SiO_2 absorbed on the surface, thus fragmentation of analyte decrease, and analyte ionize successfully in presence of high charged MALDI plume without loss of resolution.

4. Conclusions

Results from this study revealed that G@SiO_2 initiated by CTAB for high ionization efficiency and high stability. However, MALDI plume has a lot of positive charge from surfactants; it still shows high ionization, high resolution and low fragmentation of various analytes. Specifically, G@SiO_2 does not require a matrix, high ionization efficiency and low interferences. Recognize the role of surfactant/stabilizing agent that used during nanoparticles preparation may be useful to understand MALDI ion formation using nanoparticles for SALDI-MS. Unlike conventional MALDI, G@SiO_2-MS is capable of generating multiply charged polysaccharides. G@SiO_2-MS exhibits a great potential to distinguish among different isobaric biomolecules.

Appendix A. Supporting information

Supplementary data associated with this article can be found in the online version at http://dx.doi.org/10.1016/j.talanta.2014.03.016.

References

[1] K. Tanaka, H. Waki, Y. Ido, S. Akita, Y. Yoshida, T. Yoshida, Rapid Commun. Mass Spectrom. 2 (1988) 151–153.
[2] K. Strupat, M. Karas, F. Hillenkamp, Int. J. Mass Spectrom. Ion Process. 72 (1991) 89–102.
[3] R.C. Beavis, B.T. Chait, Rapid Commun. Mass Spectrom. 3 (1989) 436–439.
[4] J. Wei, J.M. Buriak, G. Siuzdak, Nature 399 (1999) 243–246.
[5] H. Kawasaki, T. Akira, T. Watanabe, K. Nozaki, T. Yonezawa, R. Arakawa, Anal. Bioanal. Chem. 395 (2009) 1423–1431.
[6] D.S. Peterson, Mass Spectrom. Rev. 26 (2007) 19–34.
[7] C.K. Chiang, W.T. Chen, H.T. Chang, Chem. Soc. Rev. 40 (2011) 1269–1281.
[8] P.A. Kuzema, Anal. Chem. 66 (2011) 1227–1242.
[9] R. Pilolli, F. Palmisano, N. Cioffi, Anal. Bioanal. Chem. 402 (2012) 601–623.
[10] H.F. Wu, J. Gopal, H.N. Abdelhamid, N. Hasan, Proteomics 12 (2012) 2949–2961.
[11] M.F Wyatt, S. Ding, B.K. Stein, A.G. Brenton, R.H. Daniels, J.Am. Soc. Mass. Spectrom. 21 (2010) 1256–1259.

[12] A. Woldegiorgis, F.V. Kieseritzky, E. Dahlstedt, J. Hellberg, T. Brinck, J. Roeraade, Rapid Commun. Mass Spectrom. 18 (2004) 841–852.
[13] Y.S. Lin, Y.C. Chen, Anal.Chem. 74 (2002) 5793–5798.
[14] Q. Zhan, S.J. Wright, R. Zenobi, J. Am. Soc. Mass Spectrom. 8 (1997) 525–531.
[15] D.M. Hrubowchak, M.H. Ervin, N. Winograd, Anal. Chem. 63 (1991) 1947–1953.
[16] Z. Guo, Q. Zhang, H. Zou, B. Guo, N. Jianyi, Anal. Chem. 74 (2002) 1637–1641.
[17] K.S. Novoselov, A.K. Geim, S.V. Morozov, D. Jiang, Y. Zhang, S.V. Dubonos, I.V. Grigorieva, A.A. Firsov, Science 306 (2004) 666–669.
[18] L.A. Tang, J. Wang, K.P. Loh, J. Am. Chem. Soc. 132 (2010) 10976–10977.
[19] X. Zhou, Y. Wei, Q. He, F. Boey, Q. Zhang, H. Zhang, Chem.Commun. 46 (2010) 6974–6976.
[20] J. Zhang, X.L. Dong, J.S. Cheng, J.H. Li, Y.S. Wang, J. Am. Soc. Mass Spectrom. 22 (2011) 1294–1298.
[21] H.N. Abdelhamid, H.F. Wu, Anal. Chim. Acta. 751 (2012) 94–104.
[22] Y. Liu, J. Liu, P. Yin, M. Gao, C. Deng, X. Zhang, J. Mass. Spectrom. 46 (2011) 804–815.
[23] L. Ai, L. Tang, J. Wang, K.P. Loh, J. Am. Chem. Soc. 132 (2010) 10976–10977.
[24] H.N. Abdelhamid, H.F. Wu, J. Am. Soc. Mass Spectrom. (2014), http://dx.doi.org/10.1007/s13361-014-0825-z.
[25] Q. Liu, J. Shi, G. Jiang, Trends Anal. Chem. 37 (2012) 1–11.
[26] H.J. Rader, A. Rouhanipour, A.M. Talarico, V.P. Samor, K. Mullen, Nat. Mater. 5 (2006) 276–279.
[27] Y.F. Lee, K.H. Chang, C.C. Hu, Y.H. Lee, J. Mater. Chem. 21 (2011) 14008–140012.
[28] W.S. Hummers, R.E. Offeman, J. Am. Chem. Soc. 80 (1958) 1339 (1339).
[29] C.W. Liang, P.J. Chang, Y.J. Lin, Y.T. Lee, C.K. Ni, Anal. Chem. 84 (2012) 3493–3499.
[30] M.L. Vestal, Chem. Rev. 101 (2001) 361–396.
[31] R. Knochenmuss, R. Zenobi, Chem. Rev. 103 (2003) 441–452.
[32] T.R. Northen, O. Yanes, M.T. Northen, D. Marrinucci, W. Uritboonthai, J. Apon, S.L. Golledge, A. Nordström, G. Siuzdak, Nature 449 (2007) 1033–1036.
[33] Q. Liu, J. Shi, J. Sun, T. Wang, L. Zeng, G. Jiang, Angew. Chem. Int. Ed. 50 (2011) 5913–5917.
[34] J.W. Liu, Q. Zhang, X.W. Chen, J.H. Wang, Chem. Eur. J. 17 (2011) 4864–4870.
[35] X. Lium, H. Zhang, G. Yu, Y. Ma, Y. Guo, Y. Liu, X. Wu, L. Meng, J. Mater. Chem. A. 1 (2013) 1875–1884.
[36] E. Olkowska, Z. Polkowska, J. Namieśnik, Chem. Rev. 111 (2011) 5667–5700.
[37] (a) E. Olkowska, Z. Polkowska, J. Namieśnik, Talanta 88 (2012) 1–13;
(b) J.T. Zhang, N. Smith, S.A. Asher, Anal. Chem. 84 (2012) 6416–6420.